CpG-containing immunostimulatory DNA sequences elicit TNF-α–dependent toxicity in rodents but not in humans

John D. Campbell,[1] Yan Cho,[1] Martyn L. Foster,[2] Holger Kanzler,[1] Melissa A. Kachura,[1] Jeremy A. Lum,[1] Marianne J. Ratcliffe,[2] Atul Sathe,[1] Andrew J. Leishman,[2] Ash Bahl,[2] Mark McHale,[2] Robert L. Coffman,[1] and Edith M. Hessel[1]

[1]Dynavax Technologies Corporation, Berkeley, California, USA. [2]AstraZeneca Research and Development Charnwood, Loughborough, United Kingdom.

CpG-containing immunostimulatory DNA sequences (ISS), which signal through TLR9, are being developed as a therapy for allergic indications and have proven to be safe and well tolerated in humans when administrated via the pulmonary route. In contrast, ISS inhalation has unexplained toxicity in rodents, which express TLR9 in monocyte/macrophage lineage cells as well as in plasmacytoid DCs (pDCs) and B cells, the principal TLR9-expressing cells in humans. We therefore investigated the mechanisms underlying this rodent-specific toxicity and its implications for humans. Mice responded to intranasally administered 1018 ISS, a representative B class ISS, with strictly TLR9-dependent toxicity, including lung inflammation and weight loss, that was fully reversible and pDC and B cell independent. Knockout mouse experiments demonstrated that ISS-induced toxicity was critically dependent on TNF-α, with IFN-α required for TNF-α induction. In contrast, human PBMCs, human alveolar macrophages, and airway-derived cells from *Ascaris suum*–allergic cynomolgus monkeys did not produce appreciable TNF-α in vitro in response to ISS stimulation. Moreover, sputum of allergic humans exposed to inhaled ISS demonstrated induction of IFN-inducible genes but minimal TNF-α induction. These data demonstrate that ISS induce rodent-specific TNF-α–dependent toxicity that is absent in humans and reflective of differential TLR9 expression patterns in rodents versus humans.

Introduction

CpG-containing immunostimulatory DNA sequences (ISS) have many potential clinical applications, both as vaccine adjuvants and as therapeutic agents. ISS has particular promise in allergic diseases, as it promotes Th1 and inhibits Th2 responses via signaling through TLR9 to induce IFN-α and, indirectly, NK cell production of IFN-γ (1–3). Initial studies in mouse models of allergic disease demonstrated that ISS given via the airways before primary allergen challenge prevents airway eosinophilia and hyperresponsiveness and stimulates allergen-specific IFN-γ responses (4, 5). Subsequent studies have also shown ISS to reverse established allergic responses in mice (6–8). Furthermore, ISS treatment resulted in reversion of lung tissue responses to inflammatory leukocyte infiltration (8). ISS acutely inhibits Th2-mediated airway inflammation by inhibiting local lung antigen-presenting cell costimulatory molecule expression and by preventing Th2 cytokine release from airway Th2 cells, basophils, and/or mast cells, highlighting the functional importance of ISS delivery to the airways (9). ISS efficacy in mouse models of asthma has been subsequently confirmed in rhesus monkeys in which inhaled ISS suppresses airway hyperresponsiveness and cellular inflammation in the lung tissue (10). Importantly, recent clinical studies have demonstrated potential for ISS-allergen conjugate therapy in human allergic airways disease (11–13).

Although the ability of ISS to inhibit allergic responses has been demonstrated in mice, monkeys, and humans, responses to ISS in vivo are qualitatively and quantitatively different between rodents and primates. This may result in species-specific toxicities in rodents that are not representative of the responses to comparable ISS treatments of humans and nonhuman primates. Indeed, inhaled or injected ISS have been shown to be safe and well tolerated in several human and nonhuman primate studies (refs. 10–15 and our unpublished observations). In contrast, ISS treatment at or above doses with therapeutic efficacy can have adverse effects in rodents. Lung inflammation — characterized by increased cellular infiltrate and elevated levels of lung and plasma inflammatory cytokines, such as TNF-α and IL-6 — has been reported in mice receiving i.t. administration of bacterial DNA or ISS (refs. 16, 17, and our unpublished observations).

The precise mechanisms underlying this interesting discrepancy in ISS responses between rodents and primates are as yet unexplained. The enhanced sensitivity of rodents to adverse toxicological effects of CpG oligonucleotide (ODN) may be a consequence of the broader pattern of cellular expression of the TLR9 receptor for CpG ODN. In humans, TLR9 expression in mononuclear blood cells and lymphoid organs is restricted to B cells and plasmacytoid DCs (pDCs), according to a consensus of the best quality data (18–20). In mice, however, TLR9 expression and ISS responsiveness have been demonstrated in macrophages, myeloid DCs (mDCs), and activated T cells in addition to pDCs and B cells (21–24). Expression of TLR9 on more diverse cell types may result in additional proinflammatory mediators being released in rodents in response to ISS compared with humans and nonhuman primates (14, 23).

While differential TLR9 expression patterns may be the basis for the different toxicological responses in rodents and primates, the specific cells and mediators responsible for those differences are poorly understood. A clear understanding of the species-specific differences in ISS responses between rodents and primates will be

essential for designing effective ISS treatment regimens for humans and will ensure that toxicology studies of ISS in rodents and nonhuman primates can be interpreted and the implications for human safety rigorously assessed. In this report, we investigated the cell types and cytokines responsible for ISS-induced toxicity in mice with ISS delivered to the airways and demonstrate that the principal toxicities observed in these animals were caused by mediators, especially TNF-α, produced prominently by monocyte/macrophage lineage cells. In primates, these cell types do not express TLR9, which resulted in TNF-α being a negligible part of the ISS response. We conclude that this fundamental difference in TLR9 expression patterns accounts for much of the exaggerated toxicity observed in rodents exposed to high doses of ISS in the respiratory tract.

Results

Delivery of high-dose ISS i.n. induces TLR9-dependent lung tissue inflammation, inflammatory cytokine production, and weight loss. In order to investigate mechanisms responsible for rodent ISS-induced toxicity, we examined i.n. ISS-treated mice for quantifiable and reproducible parameters of pathology. Lung tissue sections and BAL fluid (BALF) were harvested from C57BL/6 and *TLR9*^{−/−} mice given 1018 ISS i.n. A 5-mg/kg dose of 1018 ISS resulted in marked pulmonary inflammation in lung tissue sections from C57BL/6 mice harvested 4 days after treatment. Extensive perivascular and peribronchiolar mononuclear and neutrophilic inflammatory infiltrates were evident in H&E-stained lung tissue of ISS-treated C57BL/6 mice (Figure 1A). In addition, bronchiolitis with marked bronchiolar mucosal hyperplasia, together with associated alveolitis and pneumonitis (especially evident within the peribronchiolar zone), were also noted. In stark contrast, i.n. 1018 ISS administration to *TLR9*^{−/−} mice did not induce tissue inflammation, demonstrating the complete dependence of lung pathology on signaling through TLR9 (Figure 1A). Saline or nonstimulatory control ODN (cODN) administration to C57BL/6 or *TLR9*^{−/−} mice did not result in tissue inflammation.

The pulmonary inflammation resulting from 1018 ISS administration to C57BL/6 mice was associated with elevated levels of IFN-γ, TNF-α, IL-6, and IL-12$_{p40}$ detected in the BALF at day 4 (Figure 1B). 1018 ISS did not induce BALF cytokines in *TLR9*^{−/−} mice. TNF-α, IL-6, and IL-12$_{p40}$ were detected in BALF at 3 hours after treatment in C57BL/6 mice, while IFN-α and IFN-γ were only detectable 24 hours after dosing with 1018 ISS (Supplemental Figure 1; supplemental material available online with this article; doi:10.1172/JCI38294DS1). ISS-induced pulmonary inflammation in C57BL/6 mice was also accompanied by approximately 10% weight loss at day 1 in mice treated with 5 or 10 mg/kg 1018 ISS (Figure 1C). Less weight loss was evident in mice that received 1 or 2.5 mg/kg 1018 ISS, indicating a dose-dependent response, with reduced toxicity at doses that are optimum in mouse model therapeutic studies (9). Although C57BL/6 mice sustained 10% weight loss from day 1 to day 4 after 1018 ISS treatment, *TLR9*^{−/−} mice did not show a loss in weight in the days after 1018 ISS administration (Figure 1C). Taken together, these data demonstrate clearly that the toxicological effects consequent to airway administration of 1018 ISS in mice are strictly TLR9 dependent.

BALF cytokines, weight loss, and lung tissue inflammation induced by 1018 ISS are fully reversible. To determine whether 1018 ISS–induced toxicity was readily reversible or resulted in lasting damage to the airways, BALF cytokines, weight loss, and lung tissue inflammation were examined for up to 63 days after a single i.n.

treatment with 1018 ISS or saline in C57BL/6 mice. BALF inflammatory cytokine levels peaked at day 1 after 1018 ISS treatment and were largely undetectable by 8 days after treatment (Figure 2A). Similarly, 1018 ISS–induced weight loss was most acute at days 1 and 4 after treatment and was less marked by day 8 (Figure 2B). By day 14, 1018 ISS–treated mice were gaining weight at a rate equivalent to that of saline-treated control mice. In order to quantify the kinetics of lung tissue changes resulting from 1018 ISS airway administration, H&E-stained sections from C57BL/6 mice were assigned graded scores. A scoring scale of 1–5 was used to grade the extent of bronchiolar and lung vascular pathology, leukocyte recruitment, and inflammation-associated tissue remodeling. Mice treated with 1018 ISS demonstrated extensive leukocyte infiltration, reactive tissue pathology (e.g., bronchiolar hyperplasia), and inflammation-associated remodeling, which peaked at 8 days after treatment and declined to baseline by 28 days (Figure 2C). Mice given a single i.n. administration of saline exhibited no pulmonary pathological changes from day 1 to day 63 (data not shown). Thus, the lung tissue pathology evident in mice after a single dose of 1018 ISS was reversible, with tissue damage and remodeling changes all occurring in response to the initial leukocyte infiltration. These data demonstrated the complete reversibility of 1018 ISS–induced tissue pathology, BALF cytokine induction, and weight loss in mice.

ISS-induced mouse toxicity is not dependent on pDCs or B cells. Several reports in the literature demonstrate that TLR9 expression is restricted to pDCs and B cells in the mononuclear cell compartment of human and nonhuman primate blood, whereas in rodents the receptor is also expressed in other DC subsets, monocytes, and activated T cells (18–25). The substantial differences between rodents and primates in both the severity and the nature of the pulmonary response to ISS suggested that these differences were mediated by cell types that are ISS responsive in mice and rats, but not in monkeys and humans. Specifically, we postulated that a significant component of the inflammatory cytokine response in rodents originates from TLR9-expressing monocytes and monocyte-derived DCs.

In order to determine the mechanisms underlying the pulmonary inflammatory response to ISS in rodents, we first investigated whether either of the cell types that express TLR9 in both rodents and primates, pDCs and B cells, was necessary for the toxicological inflammatory response in rodents. pDCs were depleted in vivo in C57BL/6 mice by i.p. injection of antibody against pDC antigen–1 (PDCA-1) 24 hours prior to i.n. 1018 ISS administration. pDC-depleted mice demonstrated 10%–15% weight loss at 24 hours after 1018 ISS dosing, similar to that of mice pretreated with saline or rat IgG2b antibody (anti–PDCA-1 isotype control; Figure 3A). In addition, there were no differences in 1018 ISS–induced lung tissue pathology between the pDC-depleted and nondepleted mouse groups: median lung bronchiole and vascular pathology scores for 1018 ISS–dosed groups were 2.0 and 2.5 for anti–PDCA-1–treated, 2.0 and 2.5 for rat IgG2b–treated, and 2.5 and 3.0 for saline-treated mice. Mice administered cODN did not demonstrate weight loss, lung inflammation, or BALF cytokine induction (data not shown).

Levels of IFN-γ, IL-12$_{p40}$, and TNF-α were similar between pDC-depleted mice and controls. However, BALF IFN-α and IL-6 were significantly reduced in pDC-depleted mice (Figure 3B). pDCs are the principal source of IFN-α, consistent with the very low levels of this cytokine found in pDC-depleted mice. pDCs may also produce some IL-6 (26). Depletion of pDCs was verified by flow cytometry analysis 24 hours after anti–PDCA-1 treatment (Sup-
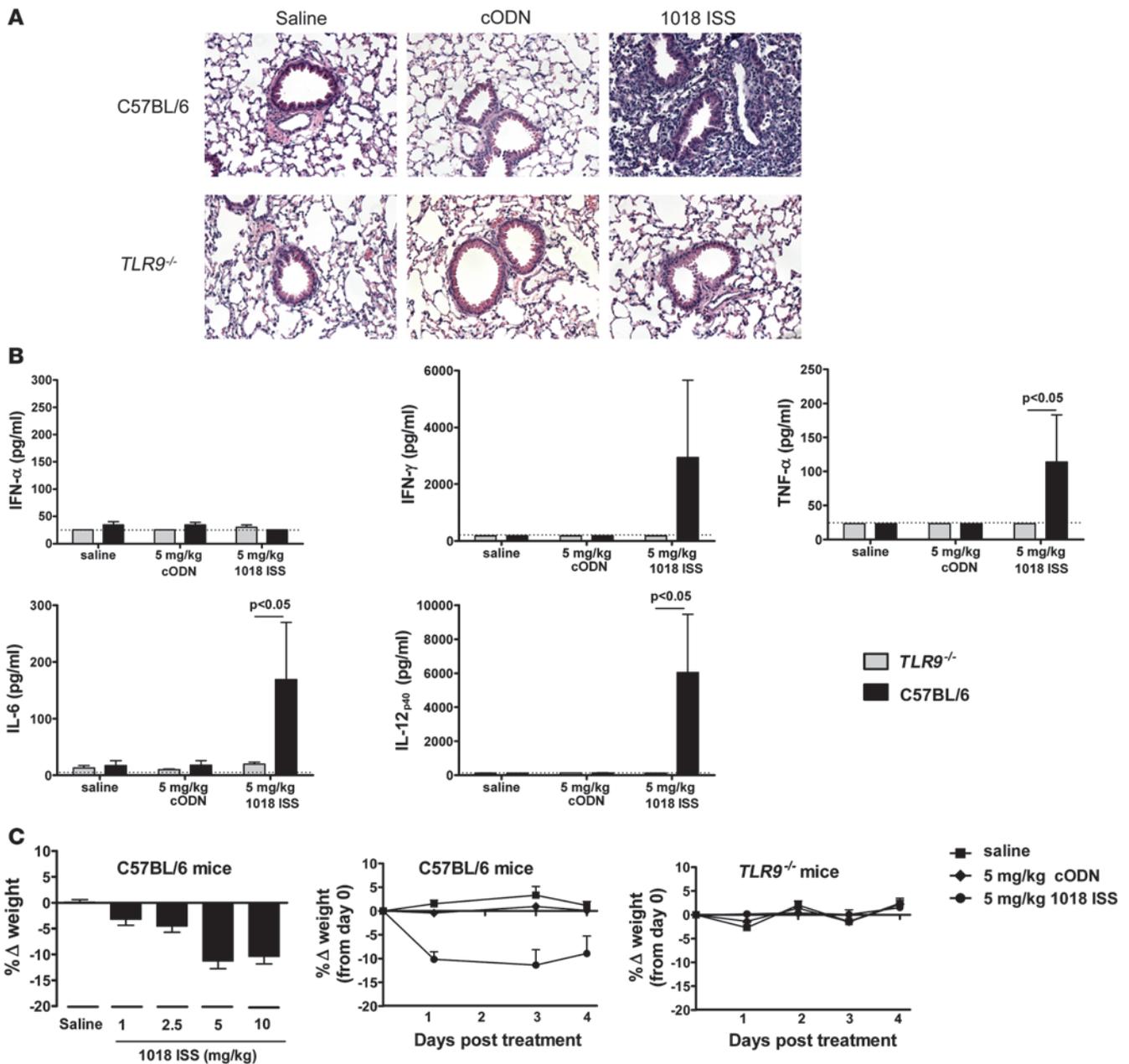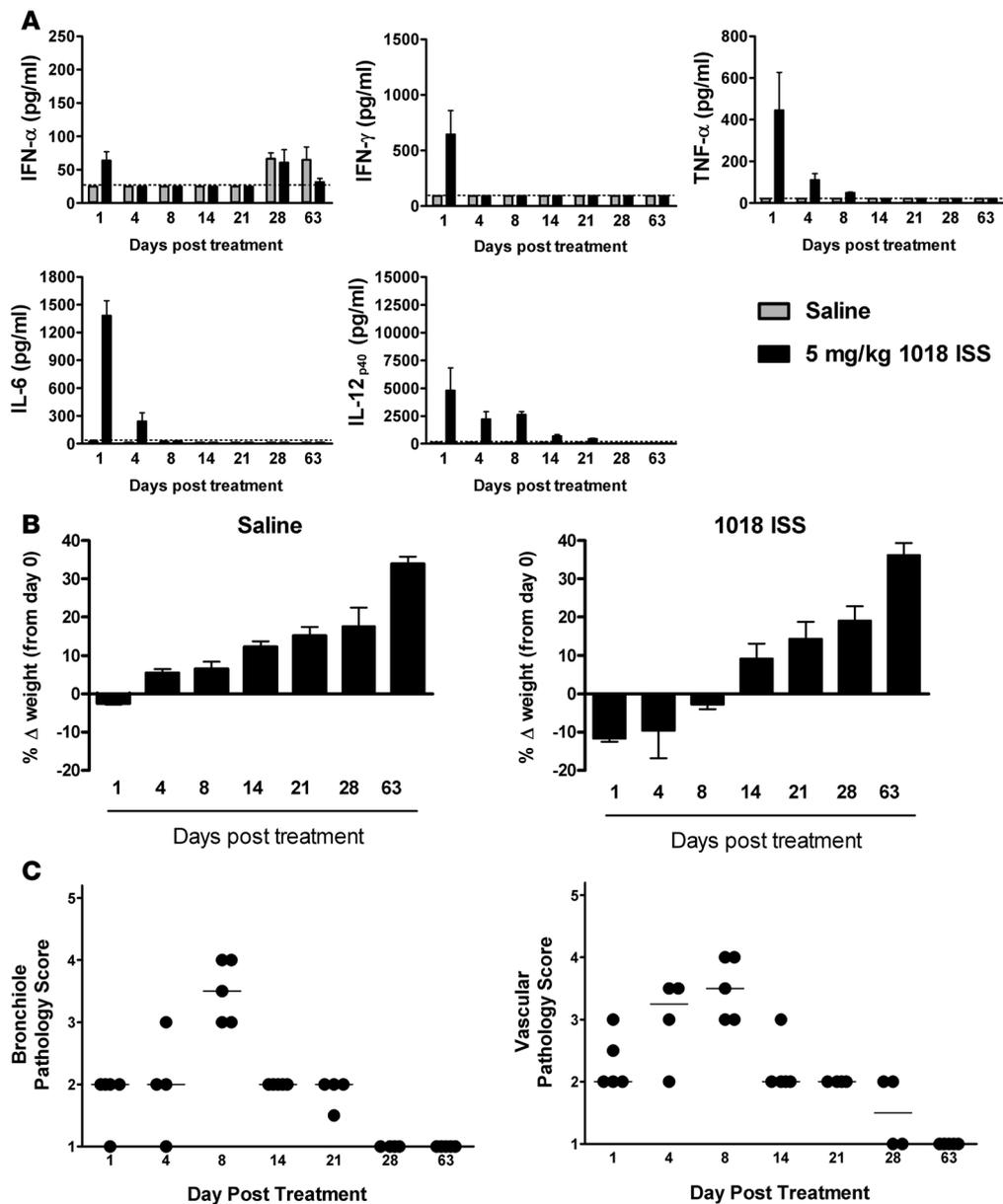
Figure 1
Delivery of 1018 ISS i.n. to C57BL/6 mice, but not *TLR9−/−* mice, results in lung tissue inflammation, release of cytokines into the lung lumen, and weight loss. Mice were dosed with 1018 ISS at 5 mg/kg, cODN at 5 mg/kg, or saline i.n. on day 0 and were euthanized at day 4. (**A**) Lung tissue samples from C57BL/6 and *TLR9−/−* mice were preserved in formalin prior to paraffin embedding and processing into 4-μm-thick sections, which were stained with H&E to visualize lung inflammation. Data are representative of 5 lungs examined per group. Original magnification, x20. (**B**) BALF cytokine levels (mean ± SEM; day 4) were quantified by ELISA. Dotted lines indicate minimum detection levels for the ELISA assay. (**C**) Mice were weighed daily after i.n. dosing, and change in weight relative to day 0 (mean ± SEM) was calculated. Weight response to i.n. 1018 ISS (1–10 mg/kg) was calculated at day 1 after dosing. *n* = 10 per group.

plemental Figure 2). Anti–PDCA-1 treatment eliminated greater than 95% of the pDC population, accounting for the highly significant reduction in IFN-α measurable in BALF. As the in vivo depletion of pDCs in excess of 95% did not measurably reduce the toxicological consequences of 1018 ISS administration, these data strongly suggest that pDCs are not required for ISS-induced toxicity in the mouse.

The role of B cells in 1018 ISS–induced toxicity was similarly assessed by treating B cell–deficient ($J_H−/−$) mice and wild-type BALB/c control mice with 1018 ISS i.n. 1018 ISS–treated B cell–deficient mice and BALB/c controls displayed similar weight loss (Figure 4A), BALF cytokine levels (Figure 4B), and pulmonary inflammation. Median lung bronchiole pathology scores were 2.0 and 3.0 for 1018 ISS–dosed wild-type and B cell–deficient mice, while a median

Figure 2
Mouse lung tissue inflammation, BALF cytokines, and body weight loss in response to a single 1018 ISS dose is fully reversible. C57BL/6 mice were treated with 5 mg/kg 1018 ISS or saline i.n., and animals were sacrificed from day 1 to 63. (**A**) BALF cytokines (mean ± SEM) were measured by ELISA. Dotted lines indicate minimum detection levels for the ELISA assay. (**B**) Mouse weight was recorded at sacrifice, and weight change compared with day 0 (mean ± SEM) was calculated. (**C**) H&E-stained lung sections were scored on a scale of 1–5 for 1018 ISS–induced tissue inflammation and pathology. Median lines are shown. n = 5 per group.

vascular pathology score of 3.0 was obtained for both wild-type and B cell–deficient mice. There was no measurable response to cODN administered i.n. in either B cell–deficient or BALB/c mice (data not shown). Thus, B cells were not required for TLR9-mediated ISS-induced toxicity in the mouse. Taken together, the data from mice depleted of pDCs or deficient for B cells indicate that ISS stimulation of these cell types through TLR9 makes little or no contribution to ISS-induced toxicity in the respiratory tract.

In mice, 1018 ISS–induced toxicity is mediated by TNF-α. The similarity of the kinetics of inflammatory cytokine induction and weight loss after 1018 ISS airway administration suggest a causal link between these responses. In order to determine the mediators involved in 1018 ISS–induced toxicity in rodents, we examined the response to i.n. delivery of 1018 ISS in a variety of cytokine and cytokine receptor knockout mice. We immediately suspected TNF-α, because it is well known as a principal mediator of cellular inflammation and weight loss accompanying inflammation (27). Indeed, high doses of 1018 ISS failed to produce significant weight loss in *TNF-α*^{-/-} mice, in contrast to the prominent weight loss in WT mice of the same genetic background (Figure 5A). Furthermore, mice lacking TNF-α exhibited markedly reduced lung pathology in response to 1018 ISS dosing. ISS-treated *TNF-α*^{-/-}
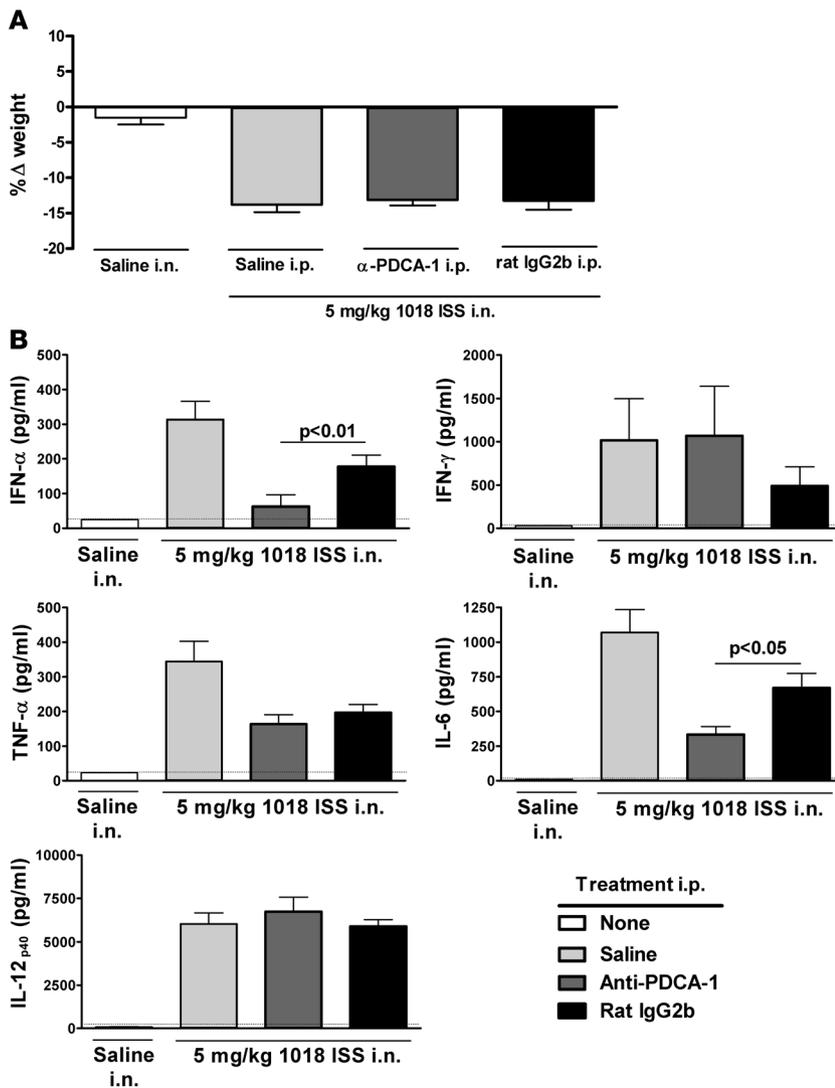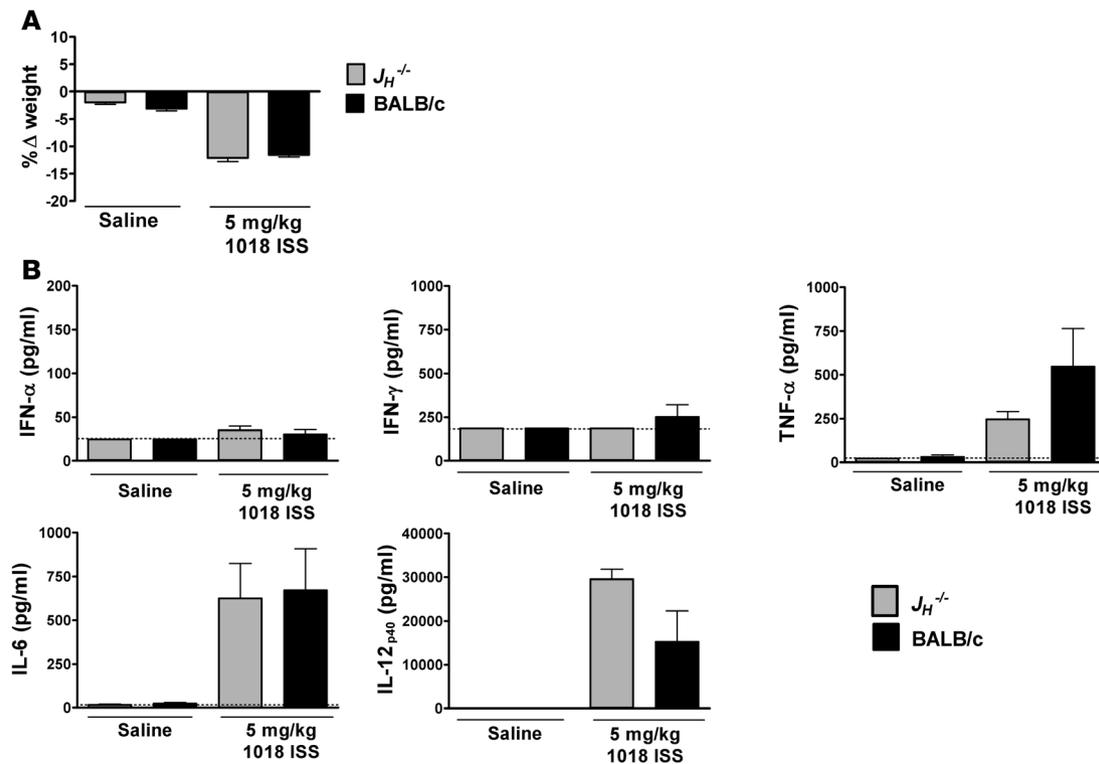
Figure 3
pDCs are not required for 1018 ISS–induced toxicity. pDC-depleted and nondepleted mice were treated with 5 mg/kg 1018 ISS or saline i.n. and sacrificed 24 hours later. Mice were depleted of pDC by i.p. injection of anti–PDCA-1 24 hours prior to i.n. administration of 1018 ISS. Rat IgG2b was used as an isotype control for the anti–PDCA-1 antibody. (**A**) Weight was measured at 1018 ISS administration and 24 hours later, and change in weight (mean ± SEM) was calculated. (**B**) BALF cytokines (mean ± SEM) were measured by ELISA. Dotted lines indicate minimum detection levels for the ELISA assay. n = 5–8 per group.

mice had a median bronchiole lung pathology score of 1.0, compared with 2.0 for wild-type mice, and lung vascular pathology scores were 1.0 and 3.0, respectively, for *TNF-α*^{−/−} and wild-type mice. These data were confirmed in *p55p75*^{−/−} mice, which lack both the p55 and the p75 TNF receptors (TNFRs). These mice exhibited no significant lung tissue pathology (median bronchiole and vascular scores, *p55p75*^{−/−}, 1.0; WT, 3.0) and did not lose weight after i.n. 1018 ISS administration (Figure 5B). In contrast, single TNFR-knockout *p75*^{−/−} and wild-type mice demonstrated similar weight loss after 1018 ISS treatment (Figure 5C). Except for the expected absence of TNF-α in BALF of 1018 ISS–treated *TNF-α*^{−/−} mice, levels of all other BALF cytokines in these mice were comparable with those of wild-type controls (Figure 5D). Treatment with cODN sequences i.n. elicited no measurable responses in any of the TNF-α– or TNFR-deficient mice or wild-type mice (data not shown). These results clearly implicate TNF-α as a central mediator of ISS-induced TLR9-mediated toxicity in the mouse. Monocytes/macrophages and DCs represent a likely source of TNF-α in 1018 ISS–treated mice. Both DCs (CD11c+ cells) and monocytes/macrophages (CD11b+ cells) from 1018 ISS–treated mice showed signification elevation of

TNF-α mRNA compared with saline-treated mice when isolated from mouse lungs 2 hours after i.n. administration of 1018 ISS (Supplemental Figure 3).

To investigate whether IFN-α also contributes to 1018 ISS–induced toxicity, we examined responses to 1018 ISS in *IFNAR*^{−/−} mice, which are unresponsive to all species of IFN-α and IFN-β. *IFNAR*^{−/−} mice did not lose weight when treated with high doses of 1018 ISS (Figure 6A) and demonstrated minimal lung tissue pathology (Figure 6B). Strikingly, apart from low levels of IL-12_{p40}, BALF cytokines were totally absent in *IFNAR*^{−/−} mice treated with i.n. 1018 ISS (Figure 6C). Responses of cODN-treated *IFNAR*^{−/−} and wild-type mice were similar to each other and to those of saline-treated mice (data not shown). These data suggest that IFNAR signaling may be involved in the induction or sustained expression of inflammatory cytokines, including TNF-α, in the mouse. Similar observations have previously been reported in experimental studies of bacterial, yeast, and viral infection in *IFNAR*^{−/−} mice (28–30).

In order to clarify further the role of inflammatory cytokines in 1018 ISS–induced toxicity, we examined responses in IL-6, IFN-γ, and IL-12Rβ2 knockout mice and mice in which IL-12_{p40} was

Figure 4
B cells are not required for 1018 ISS–induced toxicity. B cell deficient mice and wild-type controls were treated with 5 mg/kg1018 ISS or saline by the i.n. route and were sacrificed 24 hours later. (**A**) Weight was measured for B cell–deficient ($J_H^{-/-}$) and wild-type mice both at 1018 ISS administration and 24 hours later, and change in weight (mean ± SEM) was calculated. (**B**) BALF cytokines (mean ± SEM) were measured by ELISA. Dotted lines indicate minimum detection levels for the ELISA assay. n = 5–8 per group.

neutralized. All these mice displayed 1018 ISS–induced toxicological responses similar to those in control mice (Supplemental Figure 4). Thus, IL-6, IFN-γ, IL-12 p70, IL-12$_{p40}$ homodimers, or IL-23, which also contains the IL-12$_{p40}$ subunit, were not required for TLR9 pathway–mediated toxicity in the mouse. The lack of a measurable role for these other major proinflammatory cytokines further supported our conclusion that TNF-α is the crucial mediator of TLR9-mediated inflammation and weight loss in the mouse. Indeed, TLR9 agonist–induced lung pathology and inflammatory mononuclear cell infiltration, when present, displayed a consistent phenotype among all cytokine-deficient mice and control mouse strains, indicative of a common mechanistic cause (data not shown).

TNF-α levels are elevated in blood of i.n. 1018 ISS–treated mice. To confirm that TNF-α was a key mediator of 1018 ISS–induced cachexia, we examined the changes in blood TNF-α levels in1018 ISS–treated mice. Specifically, plasma TNF-α levels were measured at 1.5, 3, 6, and 24 hours after i.n. 1018 ISS treatment. TNF-α was detected in plasma at 1.5 hours, and peaked at 3 hours, after i.n. 1018 ISS treatment (Figure 7A). Thus, TNF-α was elevated both locally and systemically in response to i.n. 1018 ISS delivery in mice. Treatment with the TNF inhibitor etanercept, a soluble form of TNF receptor that neutralizes TNF in circulation, resulted in significantly less body weight loss in response to i.n. 1018 ISS compared with that in control antibody–treated mice (Figure 7B). These results confirm TNF-α as the principal mediator of high-dose i.n. 1018 ISS–induced weight loss in mice.

Human PBMCs and alveolar macrophages as well as monkey BAL cells produce minimal to no TNF-α in vitro upon stimulation with TLR9 agonists. Having demonstrated that TNF-α was the key mediator of 1018 ISS–induced toxicity in rodents, it was crucial to determine whether a similar induction of TNF-α by ISS occurs in cells from humans and nonhuman primates. PBMCs from normal, healthy donors were isolated and stimulated over large concentration ranges with 1018 ISS, cODN, the representative C class CpG ODN C274, and the TLR7/8 ligand R848 in vitro. Both 1018 ISS and C274 similarly failed to stimulate appreciable TNF-α levels from human PBMCs, while R848 stimulation resulted in strong, dose-dependent induction of TNF-α (Figure 8A). Human alveolar macrophages were of limited availability and were analyzed in a separate set of experiments excluding 1018 ISS as a stimulant. Human lung alveolar macrophages were stimulated with C274, cODN, or the TLR4 ligand LPS as a positive control. LPS induced high levels of TNF-α protein, but C274 failed to stimulate significant TNF-α production from human alveolar macrophages (Figure 8B). In contrast, mouse splenocytes responded to stimulation with CpG ODN — 1018 ISS or C274 — with high levels of TNF-α production (Figure 8C). Mouse splenocyte TNF-α responses were not affected by prior in vivo depletion of murine pDCs (data not shown). In all cases, cODN did not stimulate in vitro TNF-α production (Figure 8, A–C). Thus, agonizing TLR9 in vitro in human cellular systems with ISS resulted in minimal to no TNF-α production. We also examined ex vivo responses of BAL cells from *Ascaris suum*–allergic monkeys to 1018 ISS. In response to in vitro stimulation with a
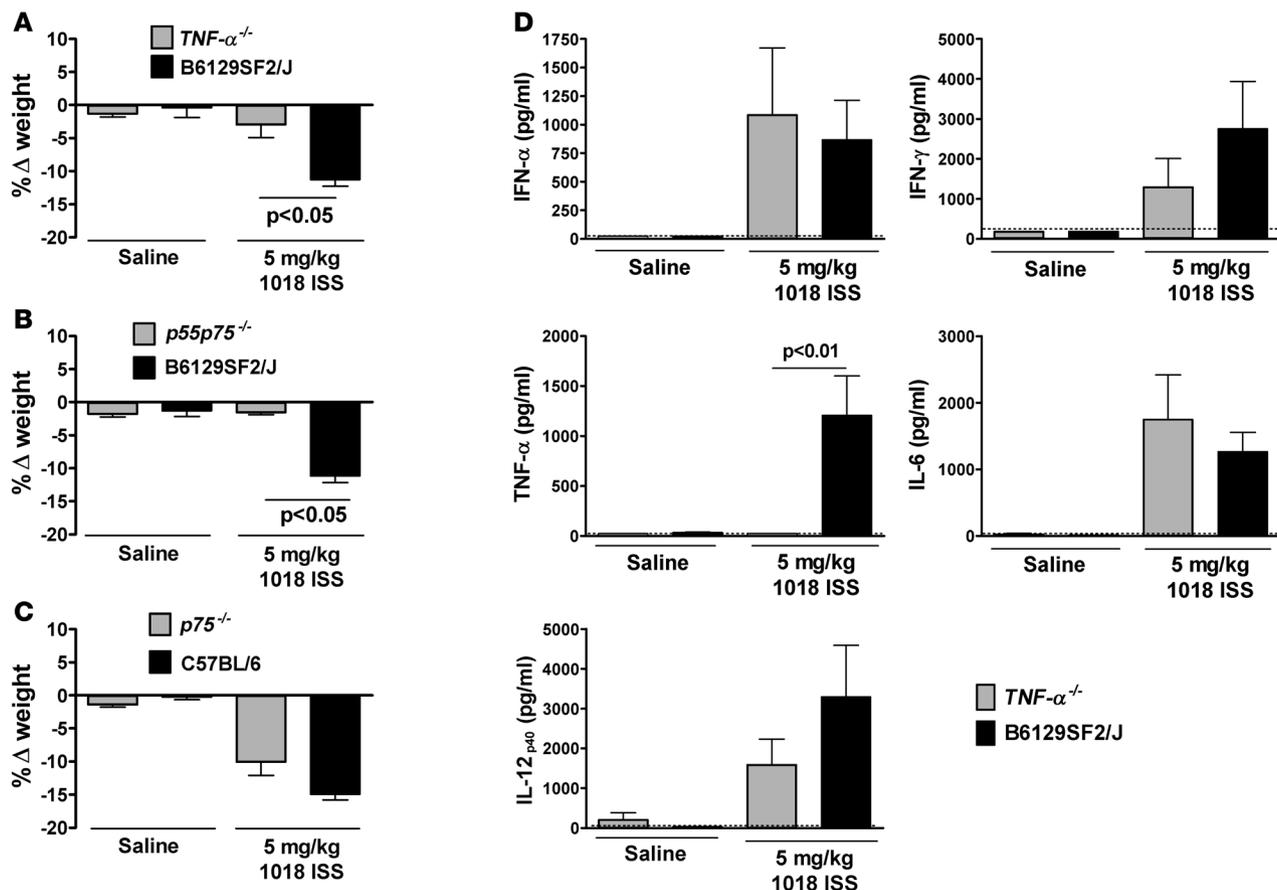
Figure 5
TNF-α is crucial for 1018 ISS–induced toxicity. Knockout and wild-type mice were treated with 5 mg/kg 1018 ISS or saline i.n. and sacrificed 24 hours later. Weight was measured for *TNF-$\alpha^{-/-}$* (**A**), *p55/p75$^{-/-}$* (**B**), and *p75$^{-/-}$* (**C**) and wild-type mice both at 1018 ISS administration and 24 hours later, and change in weight (mean ± SEM) was calculated. (**D**) BALF cytokines (mean ± SEM) in *TNF-$\alpha^{-/-}$* and wild-type mice were measured by ELISA. Dotted lines indicate minimum detection levels for the ELISA assay. $n = 5$ per group.

dose range of 0.05–3.5 μM 1018 ISS, BAL cells from allergic monkeys demonstrated minimal *TNF-α* gene expression (Figure 9A) and TNF-α protein production close to the minimum detection level (Figure 9B). R848 induced both *TNF-α* gene expression and TNF-α protein production from most monkeys, whereas cODN stimulated negligible responses. These results indicate that ISS is not a significant inducer of TNF-α from cells derived from the lungs of allergic primates.

Mildly asthmatic human subjects responded to inhalation of 1018 ISS with elevated expression of the ISS-inducible genes IP-10 and ISG-54, but not TNF-α. Inhalation delivery of 1018 ISS to human mild asthmatics has proven safe and well-tolerated with no indication of body weight loss or lung inflammation (15). This suggests that inconsequential levels of TNF-α are produced in response to TLR9 agonists in the context of human allergic disease. To confirm the relevance of our observations of minimal in vitro ISS-induced human or primate TNF-α, we directly assessed whether inhalation of ISS triggers the TNF-α pathway in allergic humans. *TNF-α* gene expression was measured in induced-sputum cells from placebo and inhaled 1018 ISS–treated donors. *TNF-α* gene expression levels were low and similar in the 1018 ISS– and placebo-treated mildly asthmatic patients ($P = 0.696$; Figure 10). In contrast, the sputum of several donors receiving inhaled 1018 ISS strongly expressed ISS-inducible

genes IFN-inducible protein of 10 kDa (*IP-10*; $P = 0.019$) and IFN-stimulated gene–54 (*ISG-54*; $P = 0.01$) compared with that of donors receiving placebo. Thus, in the context of an asthmatic lung environment in humans, 1018 ISS did not markedly trigger the TNF-α pathway. Appreciable *TNF-α* gene expression was also absent in BAL cells of healthy volunteers who inhaled 1018 ISS (data not shown). In common with treated asthmatic subjects, healthy individuals demonstrated no adverse consequences, such as weight loss or lung inflammation, after 1018 ISS inhalation. These human and primate in vitro and in vivo ISS treatment data clearly demonstrated a lack of TNF-α induction in response to TLR9 agonists. Thus, the signaling pathways triggered by TLR9 stimulation that lead to TNF-α production and subsequent mechanistic toxicity in rodents are negligible or absent in humans and primates. Taken together, our findings provide a clear mechanistic explanation for the discrepancy between the absence of TLR9 pathway–induced toxicity in humans and the presence of extensive TLR9 pathway–dependent toxicity observed in rodents.

Discussion
We have clearly defined, for the first time to our knowledge, the mechanistic basis of TLR9-mediated species-specific toxicity in the mouse. The pathogenic effects of ISS in the mouse were TLR9
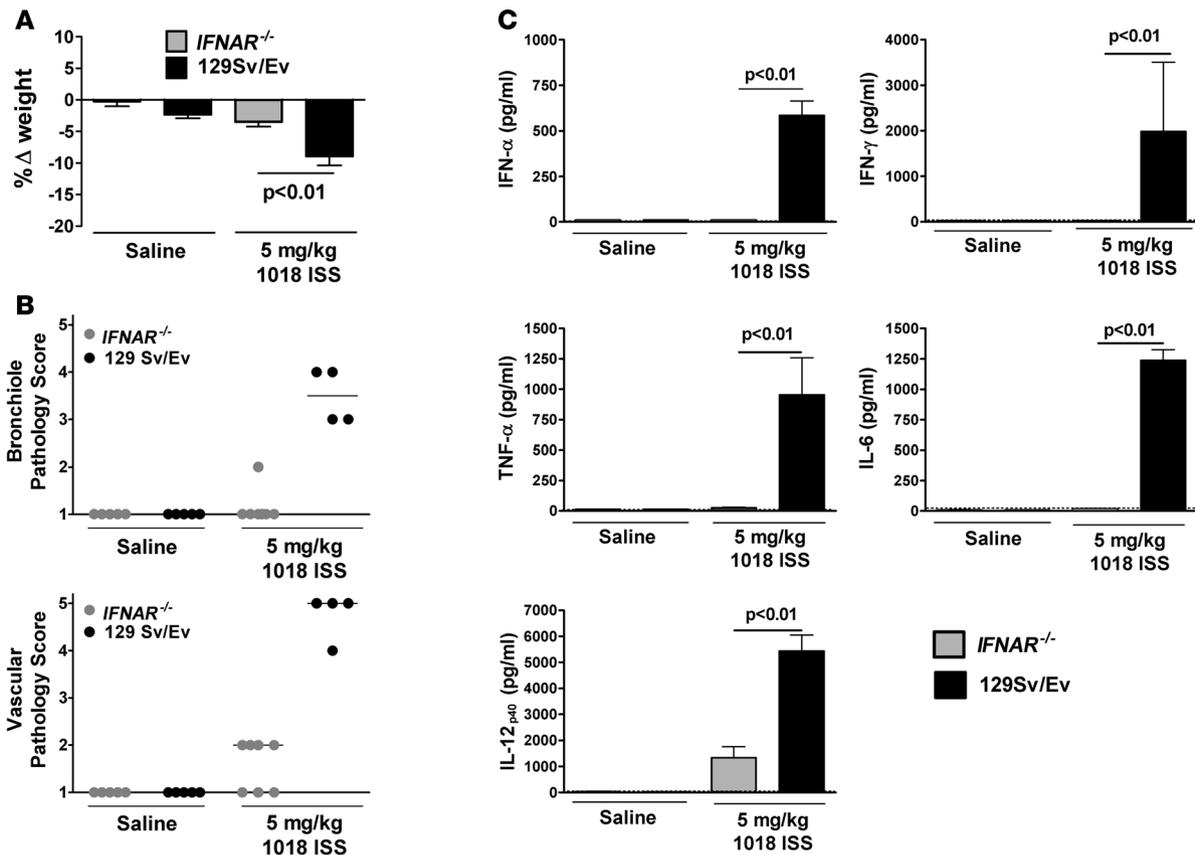
Figure 6
1018 ISS–induced toxicity is absent in *IFNAR*^{-/-} mice. Knockout and wild-type mice were treated as in Figure 5. (**A**) Weight was measured for *IFNAR*^{-/-} and wild-type mice both at 1018 ISS administration and 24 hours later, and change in weight (mean ± SEM) was calculated. (**B**) H&E-stained lung sections were scored on a scale of 1–5 for 1018 ISS–induced tissue inflammation and pathology. Median lines are shown. (**C**) BALF cytokine levels (mean ± SEM) were measured by ELISA. Dotted lines indicate minimum detection levels for the ELISA assay. $n = 5$–7 per group.

dependent, reversible, independent of pDCs and B cells, and strictly dependent on TNF-α. Thus, in rodents, 1018 ISS delivered to the lung stimulates TNF-α locally and, perhaps, systemically from cell types distinct from the principal ISS-responsive cells in humans: pDCs and B cells. TNF-α induction by i.n. ISS was prominent in mice and was crucial for the induction of lung tissue inflammation and subsequent reactive damage as well as for weight loss. In contrast, administration of an ISS aerosol to the respiratory tract of humans resulted in little or no TNF-α induction and did not lead to weight loss or evidence of pulmonary inflammation. This requirement for TNF-α and the absence of a role for pDCs and B cells suggests that the toxicity observed in mice with high doses of 1018 ISS is a rodent-specific phenomenon that is absent in humans and nonhuman primates as a result of a more restricted pattern of TLR9 expression.

The mechanistic experiments we performed in TNF-α–deficient and TNFR-deficient mice enabled us to identify TNF-α as the key mediator of 1018 ISS–induced toxicity in mice. TNF-α was also found in the circulation of mice administered i.n. 1018 ISS, and weight loss was inhibited by treatment with the TNF-α inhibitor etanercept, further confirming TNF-α–mediated toxicity. *p55p75*^{-/-} mice failed to respond to 1018 ISS with pulmonary inflammation and body weight loss, which indicates that signaling through TNF receptors was necessary for this phenomenon. *p75*^{-/-} mice were not

different from wild-type mice in their response to 1018 ISS, which suggests that TNF-α signaling through p55 was necessary for 1018 ISS–induced toxicity (although experiments were not performed with single TNFR-knockout *p55*^{-/-} mice). Whereas p55 is the principal receptor signaling biological effects of TNF-α, p75 has been previously reported to play a role in suppressing TNF-α–mediated inflammatory responses (31). However, we did not observe increased pulmonary inflammation or weight loss in *p75*^{-/-} mice.

Given the central role of IFN-α in the therapeutic effect of ISS treatment, it was important to determine its role in the toxicity of high-dose ISS therapy in mice. Monoclonal antibodies that neutralize the multiple IFN-α species in vivo are not available, and mice deficient for all IFN genes have not yet been reported. Hence, we tested ISS toxicity in *IFNAR*^{-/-} mice, which are nonresponsive to all species of IFN-α as well as to IFN-β and IFN-Ω (32). *IFNAR*^{-/-} mice did not display 1018 ISS–induced exaggerated pharmacology compared with wild-type mice. This lack of pathology correlated well with the virtual absence of inflammatory cytokines in the BALF in response to 1018 ISS. IL-12$_{p40}$ levels were substantially reduced in *IFNAR*^{-/-} mice, and TNF-α, IFN-γ, and IL-6, as well as IFN-α itself, were undetectable in these mice. A similar disruption in inflammatory cytokine responses has previously been reported in other studies with *IFNAR*^{-/-} mice. *IFNAR*^{-/-} mice produce minimal serum TNF-α in response to LPS stimulation or in response
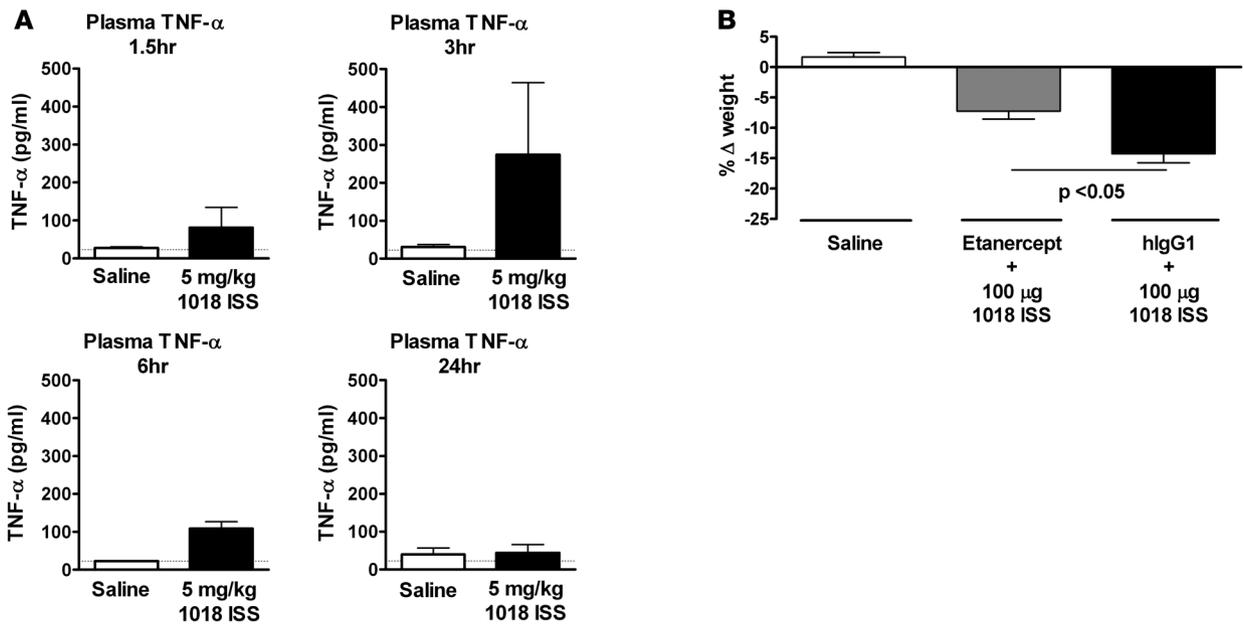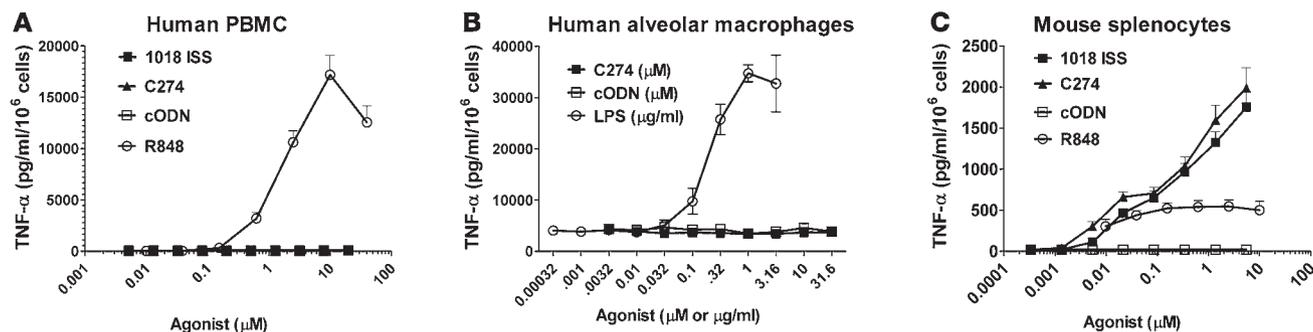
Figure 7

Kinetics of plasma TNF-α in 1018 ISS–treated mice and effect of the TNF-α inhibitor etanercept on weight loss. (**A**) Plasma was collected at 1.5, 3, 6, and 24 hours after i.n. treatment of C57BL/6 mice with 5 mg/kg 1018 ISS or saline, and plasma TNF-α protein (mean ± SEM) was quantified by ELISA. Dotted lines indicate minimum detection levels for the ELISA assay. $n = 5$ per group. (**B**) Etanercept or human IgG1 (hIgG1) isotype control antibody (both 0.5 mg/kg) was administered s.c. at 0.5 hours before ISS treatment and again 6 hours after treatment with ISS or saline. Weight was measured at the time of 1018 ISS administration and 24 hours later, and change in weight (mean ± SEM) was calculated. $n = 5$ per group.

to poly I:C–primed or vesicular stomatitis virus–primed LPS stimulation, whereas wild-type mice demonstrate high serum levels of TNF-α in response to all these stimuli (30). Resident peritoneal macrophages from $IFNAR^{-/-}$ and $IFN\text{-}\beta^{-/-}$ mice infected in vitro with group B streptococci display significantly reduced TNF-α production compared with macrophages from WT mice (28). In addition to reduced TNF-α response, bacteria- or yeast-induced IFN-γ responses are also markedly suppressed in $IFNAR^{-/-}$ mice (28, 29). Taken together with our data, these findings suggest that IFNAR signaling is necessary, but not sufficient, for TNF-α–induced toxicity in response to ISS. This helps explain the apparent discrepancy with our findings that pDC depletion did not reduce ISS-induced pathology or BALF levels of cytokines other than IFN-α and that the reduction of IFN-α was not complete (Figure 3). Thus, in pDC-depleted mice, the remaining levels of IFN-α, possibly along with IFN-β and IFN-Ω, were sufficient to support the subsequent induction of key inflammatory cytokines from non-pDC cells (33) in the lung. In humans and nonhuman primates, while the IFNAR signaling pathway is intact, induction of TNF-α does not occur because of lack of expression of TLR9 on non-pDC cells, principally macrophages and DCs (25).

Murine macrophages have previously been shown to express TLR9 and produce high levels of TNF-α after CpG ODN stimulation (34, 35). In addition, mDCs from mice express TLR9 and produce TNF-α in response to CpG ODN stimulation (36). In our present study, depletion of pDCs resulted in a significant reduction in 1018 ISS–induced BALF IFN-α and IL-6 levels, but levels of BALF TNF-α were unaffected. The absence of B cells also did not affect BALF TNF-α levels. Thus, TNF-α induced by 1018 ISS in the lung most likely arose from local macrophages or mDCs. Indeed, we found that lung monocytes/macrophages

(CD11b⁺ cells) and DCs (CD11c⁺ cells) enriched from in vivo 1018 ISS–treated mice demonstrate elevated $TNF\text{-}\alpha$ gene expression compared with cells from saline-treated lungs. One recent report, however, presented evidence that mouse alveolar macrophages do not express TLR9 and fail to respond to CpG ODN (21). At the same time, these authors showed that lung-resident mDCs do express TLR9 and respond to CpG ODN with TNF-α release. Interestingly, although the levels of TNF-α measured in BALF at 24 hours after 1018 ISS i.n. treatment varied across our experiments, the systemic weight loss observed was always within a range of 10%–15%, perhaps suggesting that a threshold range of TNF-α was sufficient to induce weight loss typical of cachexia (27). Our data demonstrated that i.n. 1018 ISS caused TNF-α–mediated local and systemic toxicity in rodents. Importantly, given the toxic effects of TNF-α, there is no evidence supporting a role for TNF-α in ISS-mediated therapy of allergic disease.

Investigation of monkey and human responses to ISS in our study indicated that TNF-α is not a major product of monkey or human cells stimulated through the TLR9 pathway. Furthermore, the mouse knockout and depletion data showed that the mouse equivalents of the principal TLR9-expressing cells in humans, pDCs and B cells, did not contribute to TNF-α–driven exaggerated pharmacology. Taken together, these data demonstrate that the toxic side effects associated with inducing TNF-α in the mouse were absent or greatly reduced in humans. This conclusion is supported by prior work demonstrating that human pDCs do not produce appreciable TNF-α in response to ISS stimulation (37, 38). In addition, human mDCs do not express TLR9 and do not release TNF-α after CpG ODN stimulation (25, 38, 39). A role for human B cells in high-level CpG ODN–induced TNF-α production is unlikely, given our results in B cell–deficient mice; how-

Figure 8
Human PBMCs and alveolar macrophages produce minimal TNF-α in response to in vitro ISS stimulation, whereas mouse splenocytes show a strong TNF-α response. (**A**) Ficoll-isolated PBMCs from normal healthy donors were stimulated with 1018 ISS, C274, cODN C661, or R848. TNF-α levels in culture supernatants (mean ± SEM) were measured by ELISA. $n = 11$ (C274); 12 (all other conditions). (**B**) Human alveolar macrophages harvested from resection tissue of lung cancer patients were stimulated with C274, cODN C661, or LPS. TNF-α levels in culture supernatants (mean ± SEM) were measured by ELISA. $n = 3$. (**C**) Splenocytes harvested from BALB/c mice were stimulated with 1018 ISS, C274, cODN C661, or R848. TNF-α levels in culture supernatants (mean ± SEM) were measured by ELISA. $n = 8$ (R848); 9 (all other conditions).

ever, these cells may produce low levels of TNF-α in response to ISS (40). Furthermore, in macaque monkeys, 1018 ISS and C274 induce very low levels of TNF-α protein (41). CpG ODN–treated rhesus PBMCs demonstrate rapid but transient *TNF-α* gene expression (42), mainly in response to CpG B-class ODN rather than A-class ODN, which may reflect B cell stimulation. TNF-α protein levels were not measured in that study. Macaque mDCs, monocyte-derived DCs, and monocytes do not express TLR9 and do not respond to CpG stimulation with TNF-α production (25). Human neutrophils have been previously reported to express TLR9, but also to produce very low levels of TNF-α — but high levels of IL-8 — in response to CpG ODN stimulation; however, this response was shown to be due to the phosphorothioate backbone of the ODN (43). Of other cell types, human eosinophils and mast cells may also express TLR9; however, production of TNF-α in these cell types in response to CpG ODN has not previously been demonstrated (44, 45). Because murine mast cells express TLR9, produce CpG ODN–stimulated TNF-α, and increase in number in the lungs of ovalbumin-challenged mice (46–48), we examined 1018 ISS–induced toxicity in mast cell–deficient mice. These mice did not demonstrate reduced 1018 ISS–induced pulmonary inflammation or body weight loss (data not shown), which suggests that mast cells were not required for the exaggerated pharmacological effects of TLR9 agonists in mice. Taken together, these data suggest that TNF-α is not produced in substantial amounts from any human cell types stimulated by ISS.

In this study, we demonstrated that mice exhibited exaggerated toxicity in the lung in response to airway-administered ISS. Furthermore, we showed that this exaggerated response to TLR9 agonism in the mouse was caused by production of TNF-α, and we propose that this is because of the additional monocytic TLR9 expression observed in the mouse (25). In stark contrast, humans and nonhuman primates have a TLR9 distribution that is restricted to B cells and pDCs. Using human PBMCs, macrophages derived from human lungs, or primate BAL cells, we demonstrated minimal TNF-α protein responses in vitro when cells were stimulated over a wide range of ISS concentrations. Recognizing that in vitro systems do not fully reproduce in vivo interactions, we confirmed that mildly asthmatic subjects given a series of inhalation doses of 1018 ISS did not demonstrate induction of *TNF-α* gene expression

in airway cells. Pharmacological activity of ISS was evident in these patients, as demonstrated by the induction of *IP-10* and *ISG-54*. Collectively, these data indicated that TLR9 agonism in the mouse results in an exaggerated pharmacological response mediated by TNF-α and thus represents species-specific mechanism–dependent toxicity. Our results are consistent with prior findings that pulmonary ISS administration is safe and well tolerated in humans and provide a mechanistic explanation for the ISS-induced toxicity in rodents observed by multiple investigators.

Methods

Ethical approval. Studies using human alveolar macrophages were approved by the National Research Ethics Service, NHS North West (Manchester, United Kingdom). The study of 1018 ISS inhalation in human subjects with mild asthma involved recruitment of subjects at 2 study sites. This study was approved by the Research Ethics Board of McMaster University (Hamilton, Ontario, Canada) and the Comité D'Ethique de la Recherche de L'Hôpital Laval, Université Laval (Sainte-Foy, Québec, Canada). Informed consent was obtained from all study subjects.

Mouse procedures were approved by the following committees: Pacific BioLabs Institutional Animal Care and Use Committee (Hercules, California, USA); Simonsen Laboratories Animal Care and Use Committee (Gilroy, California, USA); and AstraZeneca Research and Development Charnwood Project Licence Ethical Review Committee (Loughborough, United Kingdom). Animal experiments in the United Kingdom were conducted under the authority of a Home Office Project Licence in accordance with the Animal (Scientific Procedures) Act 1986. Studies using cynomolgus monkeys were approved by the Institutional Animal Care and Use Committee of Charles River Laboratories Preclinical Services (Shrewsbury, Massachusetts, USA).

Animals. TLR9$^{-/-}$ and C57BL/6 mouse colonies were maintained at Simonsen Laboratories. IFNAR$^{-/-}$ and 129 Sv/Ev mice were purchased from B & K Universal and maintained at AstraZeneca. All other mouse strains were maintained at Pacific BioLabs. B cell–deficient [C.129(B6)-*IgH-J* ^{tm1Dhu} N?+N2] and BALB/c mice were purchased from Taconic. *TNF-α$^{-/-}$* (B6;129S6-*Tnf^{tm1Gkl}*/J), *p55/p75$^{-/-}$* (B6;129S-*Tnfrsf1a^{tm11mx} Tnfrsf1b^{tm11mx}*/J), *p75$^{-/-}$* (B6.129S2-*Tnfrsf1b^{tm1Mwm}*/J), *IL-6$^{-/-}$* (B6.129S2-*Il6^{tm1Kopf}*/J), *IFN-γ$^{-/-}$* (B6.129S7-*Ifng^{tm1Ts}*/J), and B6129SF2/J (Jax #101045) mice were purchased from Jackson. C57BL/6 mice were also purchased from Charles River and Jackson, when required, as wild-type controls. Mice ranged in age from 8 to 12 weeks, were in good health, and were caged
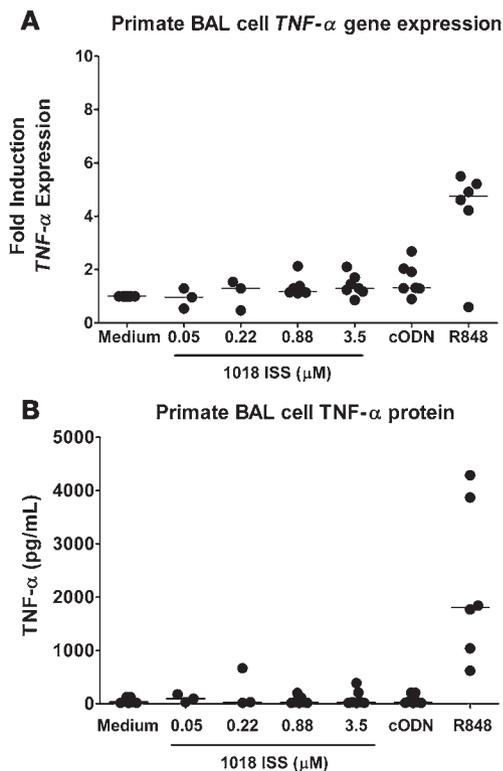
A

Primate BAL cell *TNF-α* gene expression

B

Primate BAL cell TNF-α protein

Figure 9
BAL cells from *A. suum*–allergic cynomolgus monkeys express and produce very low levels of TNF-α in response to ISS stimulation in vitro compared with the response to R848 stimulation. BAL cells isolated from *A. suum*–sensitized and allergen-challenged monkeys were stimulated with the indicated doses of 1018 ISS, with 3.5 μM cODN C661, or with 10 μM R848 as a positive control for 6 hours prior to (**A**) gene expression analysis or (**B**) culture supernatant harvest. *TNF-α* gene levels are expressed as fold induction over stimulation with medium. TNF-α levels in culture supernatants were measured by ELISA. Median lines are shown. *n* = 6.

BALF and lung tissue processing. Mice were weighed and sacrificed under CO_2 24 hours after i.n. ISS treatment (unless otherwise indicated). BALF was obtained by tracheal cannulation followed by lavage of the lungs with 1 ml sterile saline and 3 additional washes with 1 ml saline. BALF from each individual mouse was centrifuged to remove cells, lyophilized, resuspended in 200 μl saline, and stored at –80°C. Right apical lung tissue was preserved in formalin and embedded in paraffin, and 4- to 5-μM sections were stained with H&E. For preparation of single-cell suspensions, lung tissue was finely minced and incubated with 0.02 mg/ml DNase I (Sigma-Aldrich) and 1 mg/ml collagenase D (Roche) for 30 minute at 37°C with shaking. Red blood cells were lysed, and cells were thoroughly washed and plated for 1 hour at 37°C to remove adherent cells. In select experiments, CD11b+ and CD11c+ cells were enriched from single-cell suspensions of lung cells using magnetic beads from Miltenyi Biotec. Single-cell suspensions of mouse splenocytes were prepared by crushing and washing spleens through a 0.22-μM filter and lysing red blood cells.

BAL cells were obtained from *A. suum*–allergic cynomolgus monkeys under general anesthetic. Tracheal cannulation using an endoscope was performed, followed by lavage of the lungs with 20 ml sterile saline a total of 3 times. BALF from each individual monkey was centrifuged to pellet cells, red blood cells were lysed, and cells were thoroughly washed prior to plating for cell stimulations.

Human sputum. Sputum was induced and processed as described previously (15). Aliquots of cells were lysed for quantitative PCR measurements.

In vitro cell stimulations. Cell stimulations were performed in 96-well plates (200 μl total volume/well). Mouse splenocytes were cultured in RPMI medium supplemented with 10% FCS, penicillin/streptomycin, L-glutamine, HEPES buffer, sodium pyruvate, and 2-β-mercaptoethanol. Splenocytes (700,000 cells/well) were stimulated for 21–24 hours with 1018 ISS, cODN C661, or the TLR7/8 agonist R848 prior to supernatant harvest. PBMCs from healthy human donors were isolated from buffy coats by Ficoll-Histopaque. PBMCs (500,000 cells/well) were stimulated in RPMI medium without 2-β-mercaptoethanol for 24 hours, and supernatants were saved

in groups of 5–8. Male and female mice were used. A colony of purpose-bred cynomolgus monkeys was maintained at Charles River Laboratories. Monkeys were individually or pair housed and regularly screened by veterinarians for health status.

In vivo treatments. Mice were weighed, anesthetized with isoflurane, and dosed i.n. with 5 mg/kg ISS (unless otherwise noted) in 50 μl pyrogen-free saline (Sigma-Aldrich). The CpG-containing (underline) 1018 ISS (5′-TGACTGTGAA<u>CG</u>TT<u>CG</u>AGATGA) and C274 (5′-T<u>CG</u>T<u>CG</u>AA-<u>CG</u>TT<u>CG</u>AGATGAT) and non–CpG-containing cODN 1040 (5′-TGACT-GTGAACCTTAGAGATGA) and C661 (5′-TGCTTGCAAGCTTGCAAGCA) were used in this study. All sequences demonstrated less than 5 endotoxin units/mg ODN as determined by Limulus amebocyte lysate assay (Lonza). ODN sequences were synthesized as previously described (49). In certain experiments, pDCs were depleted in vivo by i.p. injection of mice with 500 μg anti–PDCA-1 (Miltenyi Biotec) 24 hours before i.n. ISS administration. IL-12$_{p40}$ was neutralized in vivo by i.p. injection of 500 μg anti-IL-12$_{p40}$ (eBioScience) 2 hours prior to i.n. ISS administration. Etanercept (Immunex) was administered at 0.5 mg/kg 30 minutes prior to ISS treatment and again 6 hours after ISS treatment. Cynomolgus monkeys were selected on the basis of positive bronchoconstrictor responses and the presence of BAL eosinophilia in response to inhaled *A. suum* antigen challenge (50).
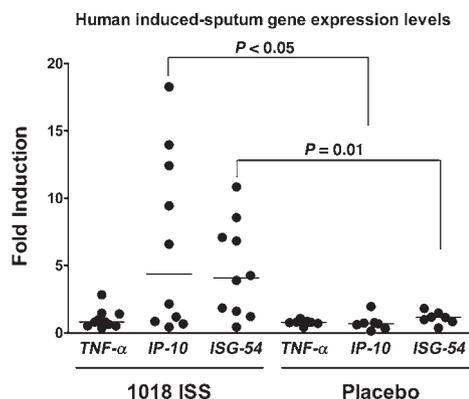
Figure 10
TNF-α is not expressed in induced sputum from mildly asthmatic patients given 1018 ISS via inhalation. Sputum of allergen-challenged and 1018 ISS–treated humans was analyzed for gene expression of *TNF-α*, *IP-10*, and *ISG-54* 24 hours after ISS inhalation. Data are expressed as fold induction of after-inhalation over pre-inhalation values. TNF-α was not induced by 1018 ISS inhalation compared with placebo inhalation (*P* = 0.6961). In contrast, 1018 ISS inhalation significantly upregulated expression of the ISS-inducible genes *IP-10* and *ISG-54*. Median lines are shown. *n* = 10.

Human induced-sputum gene expression levels

for cytokine measurement. Human alveolar macrophages were obtained from resection tissue of lung cancer patients (provided by the Midlands Lung Tissue Consortium) as previously described (51). Cells (50,000 per well) were incubated in RPMI medium (supplemented with 10% FCS, L-glutamine, and penicillin/streptomycin) in the presence of C274, cODN C661, or LPS (InvivoGen) for 18 hours prior to supernatant harvest. BAL cells from cynomolgus monkeys were cultured at 400,000 cells/ml in RPMI medium (supplemented with 10% FCS, L-glutamine, HEPES buffer, and sodium pyruvate). BAL cells were stimulated for 6 hours with 1018 ISS, cODN C661, or R848 prior to supernatant harvest.

Histological analysis of lung inflammation and tissue pathology. H&E-stained sections were examined and graded on a scale of 1–5, reflecting the severity of pathology in the bronchiolar and vascular compartments. In the case of bronchiolar pathology, low grades of 2 and 3 reflected occupation of the peribronchiolar zone and lamina propria by leukocyte infiltration, and high grades of 4 and 5 reflected reactive changes in the mucosa (such as epithelial and goblet hyperplasia and epithelial loss) and loss of wall integrity. In the case of vessel pathology, low grades reflected leukocyte occupation of the vessel wall and adventitia, and high grades were associated with frank vasculitis and loss of wall integrity. In assessing lung pathology, attention was also paid to the alveolar compartment, although weighting was given to the perivascular and peribronchiolar zones. In general, the most common pathologies of the alveolar compartment were associated with the leukocyte cuffing response around the bronchiolar and vessel adventitia and the regions of focal alveolitis and pneumonitis associated with this response. A total of 10–20 bronchioles or blood vessel sections was examined per score assigned.

ELISA. Cytokines were measured by ELISA according to the respective manufacturers' guidelines. Mouse IL-6 (detection limit, 8 pg/ml), IFN-γ (detection limit, 94 pg/ml), and TNF-α (detection limit, 23 pg/ml) were measured with R&D reagents. TNF-α levels in cultures of mouse splenocytes were quantified using Invitrogen reagents (detection limit, 8 pg/ml). IFN-α (detection limit, 25 pg/ml) was measured using a PBL Biomedical Laboratories kit. IL-12$_{p40}$ was quantified with reagents from BD Biosciences (detection limit, 63 pg/ml). Human alveolar macrophage and PBMC supernatant TNF-α levels were quantified using an optEIA ELISA kit from BD Biosciences (detection limit, 7.8 pg/ml) and cytoset antibodies from Invitrogen (detection limit, 15.6 pg/ml), respectively. Monkey TNF-α was quantified using paired antibodies from U-Cytech (detection limit, 16 pg/ml).

Real-time PCR quantification of gene expression. Both the protocol followed for analysis of gene expression and the details of sputum sample acquisition have been previously published (15). Briefly, total RNA was extracted from cells and converted to cDNA. A Bio-Rad MyIQ Single Color Real Time PCR Detection System iCycler was used for PCR reactions. The intercalating dye SYBR green (Invitrogen) was used to detect PCR product at each cycle, and cycle threshold values were determined. PCR amplification of the housekeeping gene ubiquitin was performed for each sample, allowing for normalization of data. Using normalized data, fold induction over saline treatment (mouse data), medium stimulation (monkey data), or pre–ISS treatment time point (human data) was calculated.

Flow cytometry. Analysis of pDC depletion was performed using a BD FACSCalibur (BD Biosciences). Lung-derived cells were phenotyped by staining with a variety of fluorescent-conjugated monoclonal antibodies directed against cell surface molecules. Antibodies against mouse CD3 (145-2C11), CD19 (1D3), CD49b (DX5), B220 (RA3-6B2), GR1 (RB6-8C5), and CD11c (HL3) were purchased from BD Biosciences. Anti-mouse PDCA-1 (JF05-1C2.4.1) was purchased from Miltenyi Biotec.

Statistics. Data sets were analyzed using Mann-Whitney U test. A P value less than 0.05 was considered significant.

Acknowledgments

Address correspondence to: Edith M. Hessel or John D. Campbell, Dynavax Technologies Corporation, 2929 Seventh St., Ste. 100, Berkeley, California 94710, USA. Phone: (510) 665-7255; Fax: (510) 848-1327; E-mail: EHessel@dynavax.com (E.M. Hessel). Phone: (510) 665-7281; Fax: (510) 848-1327; E-mail: DCampbell@dynavax.com (J.D. Campbell).

1. Hemmi, H., et al. 2000. A Toll-like receptor recognizes bacterial DNA. *Nature*. **408**:740–745.
2. Krieg, A.M. 2006. Therapeutic potential of Toll-like receptor 9 activation. *Nat. Rev. Drug Discov.* **5**:471–484.
3. Marshall, J.D., Heeke, D.S., Abbate, C., Yee, P., and Van Nest, G. 2006. Induction of interferon-gamma from natural killer cells by immunostimulatory CpG DNA is mediated through plasmacytoid-dendritic-cell-produced interferon-alpha and tumour necrosis factor-alpha. *Immunology*. **117**:38–46.
4. Broide, D., et al. 1998. Immunostimulatory DNA sequences inhibit IL-5, eosinophilic inflammation and airway hyperresponsiveness in mice. *J. Immunol.* **161**:7054–7062.
5. Sur, S., et al. 1999. Long term prevention of allergic lung inflammation in a mouse model of asthma by CpG oligodeoxynucleotides. *J. Immunol.* **162**:6284–6293.
6. Serebrisky, D., et al. 2000. CpG oligodeoxynucleotides can reverse Th2-associated allergic airway responses and alter the B7.1/B7.2 expression in a murine model of asthma. *J. Immunol.* **165**:5906–5912.
7. Jain, V.V., et al. 2002. CpG-oligodeoxynucleotides inhibit airway remodeling in a murine model of chronic asthma. *J. Allergy Clin. Immunol.* **110**:867–872.
8. Kline, J.N., Kitagaki, K., Businga, T.R., Jain, V.V. 2002. Treatment of established asthma in a murine model using CpG oligodeoxynucleotides. *Am. J. Physiol. Lung Cell Mol. Physiol.* **283**:L170–L179.
9. Hessel, E.M., et al. 2005. Immunostimulatory oligonucleotides block allergic lung inflammation by inhibiting Th2 cell activation and IgE-mediated cytokine induction. *J. Exp. Med.* **202**:1563–1573.
10. Fanucchi, M.V., et al. 2004. Immunostimulatory oligonucleotides attenuate airways remodeling in allergic monkeys. *Am. J. Respir. Crit. Care Med.* **170**:1153–1157.
11. Tulic, M.K., et al. 2004. Amb a 1-immunostimulatory oligodeoxynucleotide conjugate immunotherapy decreases the nasal inflammatory response. *J. Allergy Clin. Immunol.* **113**:235–241.
12. Simons, F.E.R., Shikishima, Y., Van Nest, G., Eiden, J.J., and HayGlass, K.T. 2004. Selective immune redirection in humans with ragweed allergy by injecting Amb a 1 linked to immunostimulatory DNA. *J. Allergy Clin. Immunol.* **113**:1144–1151.
13. Creticos, P.S., et al. 2006. Immunotherapy with a ragweed-toll-like receptor 9 agonist vaccine for allergic rhinitis. *N. Engl. J. Med.* **355**:1445–1455.
14. Krieg, A.M., Efler, S.M., Wittpoth, M., Al Adhami, M.J., and Davis, H.L. 2004. Induction of systemic Th1-like innate immunity in normal volunteers following subcutaneous but not intravenous administration of CpG 7909, a synthetic B-class CpG oligodeoxynucleotide TLR9 agonist. *J. Immunother.* **27**:460–471.
15. Gauvreau, G.M., Hessel, E.M., Boulet, L-P., Coffman, R.L., and O'Byrne, P.M. 2006. Immunostimulatory sequences regulate interferon-inducible geness but not allergic airway responses. *Am. J. Respir. Crit. Care Med.* **174**:15–20.
16. Schwartz, D.A., et al. 1997. CpG motifs in bacterial DNA cause inflammation in the lower respiratory tract. *J. Clin. Invest.* **100**:68–73.
17. Knuefermann, P., et al. 2007. CpG oligonucleotide activates Toll-like receptor 9 and causes lung inflammation in vivo. *Respir. Res.* **8**:72–80.
18. Hornung, V., et al. 2002. Quantitative expression of Toll-like receptor 1-10 mRNA in cellular subsets of human peripheral blood mononuclear cells and sensitivity to CpG oligodeoxynucleotides. *J. Immunol.* **168**:4531–4537.
19. Bernasconi, N.L., Onai, N., and Lanzavecchia, A. 2003. A role for Toll-like receptors in acquired

immunity: up-regulation of TLR-9 by BCR triggering in naïve B cells and constitutive expression in memory B cells. *Blood.* **101**:4500–4504.

20. Rothenfusser, S., Tuma, E., Endres, S., and Hartmann, G. 2002. Plasmacytoid dendritic cells: the key to CpG. *Hum. Immunol.* **63**:1111–1119.

21. Suzuki, K., et al. 2005. Impaired Toll-like receptor 9 expression in alveolar macrophages with no sensitivity to CpG DNA. *Am. J. Respir. Crit. Care Med.* **171**:707–713.

22. Martin-Orozco, E., et al. 1999. Enhancement of antigen-presenting cell surface molecules involved in cognate interactions by immunostimulatory DNA sequences. *Int. Immunol.* **11**:1111–1118.

23. Gilliet, M., et al. 2002. The development of murine plasmacytoid dendritic cell precursors is differentially regulated by FLT3-ligand and granulocyte/macrophage colony-stimulating factor. *J. Exp. Med.* **195**:953–958.

24. Gelman, A.E., Zhang, J., Choi, Y., and Turka, L.A. 2004. Toll-like receptor ligands directly promote activated CD4+ T cell survival. *J. Immunol.* **172**:6065–6073.

25. Ketloy, C., et al. 2008. Expression and function of Toll-like receptors on dendritic cells and other antigen-presenting cells from non-human primates. *Vet. Immunol. Immunopathol.* **125**:18–30.

26. Lenz, P., Lowy, D.R., and Schiller, J.T. 2005. Papilloma virus-like particles induce cytokines characteristic of innate immune responses in plasmacytoid dendritic cells. *Eur. J. Immunol.* **35**:1548–1556.

27. Tracey, K.J., and Cerami, A. 1990. Metabolic responses to cachectin/TNF-α. *Ann. N. Y. Acad. Sci.* **587**:325–331.

28. Mancuso, G., et al. 2007. Type 1 IFN signaling is crucial for host resistance against different species of pathogenic bacteria. *J. Immunol.* **178**:3126–3133.

29. Biondo, C., et al. 2008. IFN-α/β signaling is required for polarization of cytokine responses toward a protective type 1 pattern during experimental cryptococcosis. *J. Immunol.* **181**:566–573.

30. Nansen, A., and Thomsen, A.R. 2001. Viral infection causes rapid sensitization to lipopolysaccharide: central role of IFN-α/β. *J. Immunol.* **166**:982–988.

31. Peschon, J.J., et al. 1998. TNF receptor-deficient mice reveal divergent roles for p55 and p75 in several models of inflammation. *J. Immunol.* **160**:943–952.

32. Muller, U., et al. 1994. Functional role of type I and type II interferons in antiviral defense. *Science.* **264**:1918–1921.

33. Schroder, K., et al. 2007. Differential effects of CpG DNA on IFN-β induction and STAT1 activation in murine macrophages versus dendritic cells: alternatively activated STAT1 negatively regulates TLR signaling in macrophages. *J. Immunol.* **179**:3495–3503.

34. Sparwasser, T., et al. 1997. Macrophages sense pathogens via DNA motifs: induction of tumor necrosis factor alpha-mediated shock. *Eur. J. Immunol.* **27**:1671–1679.

35. Sweet, M.J., et al. 2002. Colony-stimulating factor-1 suppresses responses to CpG DNA and expression of Toll-like receptor 9 but enhances responses to lipopolysaccharide in murine macrophages. *J. Immunol.* **168**:392–399.

36. Edwards, A.D., et al. 2003. Toll-like receptor expression in murine DC subsets: lack of TLR7 expression by CD8 alpha+ DC correlates with unresponsiveness to imidazoquinolines. *Eur. J. Immunol.* **33**:827–833.

37. Kadowaki, N., et al. 2001. Subsets of human dendritic cell precursors express different Toll-like receptors and respond to different microbial antigens. *J. Exp. Med.* **194**:863–870.

38. Krug, A., et al. 2001. Toll-like receptor expression reveals CpG DNA as a unique microbial stimulus for plasmacytoid dendritic cells which synergizes with CD40 ligand to induce high amounts of IL-12. *Eur. J. Immunol.* **31**:3026–3037.

39. Demedts, I.K., Bracke, K.R., Maes, T., Joos, G.F., and Brusselle, G.C. 2006. Different roles for human lung dendritic cell subsets in pulmonary immune defense mechanisms. *Am. J. Respir. Cell Mol. Biol.* **35**:387–393.

40. Bohle, B., Orel, L., Kraft, D., and Ebner, C. 2001. Oligodeoxynucleotides containing CpG motifs induce low levels of TNF-α in human B lymphocytes: possible adjuvants for Th1 responses. *J. Immunol.* **166**:3743–3748.

41. Teleshova, N., et al. 2006. Local and systemic effects of intranodally injected CpG-C immunostimulatory-oligodeoxyribonucleotides in macaques. *J. Immunol.* **177**:8531–8541.

42. Abel, K., et al. 2005. Deoxycytidyl-deoxyguanosine oligonucleotide classes A, B and C induce distinct cytokine gene expression patterns in rhesus monkey peripheral blood mononuclear cells and distinct alpha interferon responses in TLR9-expressing rhesus monkey plasmacytoid dendritic cells. *Clin. Diagn. Lab. Immunol.* **12**:606–621.

43. Jozsef, L., Khreiss, T., Kebir, D.E., and Filep, J.G. 2006. Activation of TLR-9 induces IL-8 secretion through peroxynitrite signaling in human neutrophils. *J. Immunol.* **176**:1195–1202.

44. Wong, C.K., Cheung, F.Y., Ip, W.K., and Lam, C.W.K. 2007. Intracellular signaling mechanisms regulating Toll-like receptor-mediated activation of eosinophils. *Am. J. Respir. Cell Mol. Biol.* **37**:85–96.

45. Sundstrom, J.B., Little, D.M., Villinger, F., Ellis, J.E., and Ansari, A.A. 2004. Signaling through Toll-like receptors triggers HIV-1 replication in latently infected mast cells. *J. Immunol.* **172**:4391–4401.

46. Zhu, F-G., and Marshall, J.S. 2001. CpG-containing oligodeoxynucleotides induce TNF-α and IL-6 production but not degranulation from murine bone marrow-derived mast cells. *J. Leukoc. Biol.* **69**:253–262.

47. Matsushima, H., Yamada, N., Matsue, H., and Shimada, S. 2004. TLR3-, TLR7-, and TLR9-mediated production of proinflammatory cytokines and chemokines from murine connective tissue type skin-derived mast cells but not from bone marrow-derived mast cells. *J. Immunol.* **173**:531–541.

48. Ikeda, R.K., et al. 2003. Accumulation of peribronchial mast cells in a mouse model of ovalbumin allergen induced chronic airway inflammation: modulation by immunostimulatory DNA sequences. *J. Immunol.* **171**:4860–4867.

49. Fearon, K., et al. 2003. A minimal human immunostimulatory CpG motif that potently induces IFN-gamma and IFN-alpha production. *Eur. J. Immunol.* **33**:2114–2122.

50. Hart, T.K., et al. 2001. Preclinical efficacy and safety of mepolizumab (SB-240563), a humanized monoclonal antibody to IL-5, in cynomolgus monkeys. *J. Allergy Clin. Immunol.* **108**:250–257.

51. Ratcliffe, M.J., Walding, A., Shelton, P.A., Flaherty, A., and Dougall, I.G. 2007. Activation of E-prostanoid4 and E-prostanoid2 receptors inhibits TNF-α release from human alveolar macrophages. *Eur. Respir. J.* **29**:986–994.